

Atomic Force Microscopy Study of Early Morphological Changes during Apoptosis

Jessica A. Hessler,[†] Andrew Budor,[†] Krishna Puthakayala,[†] Almut Mecke,[‡]
Daniel Rieger,[†] Mark M. Banaszak Holl,^{*,†,§,||} and Bradford G. Orr^{*,‡,§}

Departments of Chemistry and Physics, Programs in Applied Physics and Biophysics, and the Michigan Nanotechnology Institute for Medicine and Biological Sciences, University of Michigan, Ann Arbor, Michigan 48109-1055

Anna Bielinska, James Beals, and James Baker, Jr.

Department of Internal Medicine and the Michigan Nanotechnology Institute for Medicine and Biological Sciences, University of Michigan Medical School, 9240 MSRB III, Ann Arbor, Michigan 48109-0666

Received July 7, 2005

Apoptosis is defined by a distinct set of morphological changes observed during cell death including loss of focal adhesions, the formation of cell membrane buds or blebs, and a decrease in total cell volume. Recent studies suggest that these dramatic morphological changes, particularly apoptotic volume decrease (AVD), are an early prerequisite to apoptosis and precede key biochemical time-points. Here we use atomic force microscopy to observe early stage AVD of KB cells undergoing staurosporine-induced apoptosis. After a 3-h exposure to 1 μ M staurosporine, a 32% decrease in total cell height and a 50% loss of total cell volume is observed accompanied by only a 15% change in cell diameter. The observed AVD precedes key biochemical hallmarks of apoptosis such as loss of mitochondrial membrane potential, phosphatidyl serine translocation, nuclear fragmentation, and measurable caspase-3 activity. This suggests that morphological volume changes occur very early in the induction of apoptosis.

Introduction

Apoptosis is defined by a distinct set of morphological changes observed during cell death including loss of focal adhesions, the formation of cell membrane buds or blebs, and a decrease in total cell volume.^{1–4} Recent studies suggest that these dramatic morphological changes, particularly apoptotic volume decrease (AVD), are an early prerequisite to apoptosis and precede key biochemical time-points.^{5–12} Atomic force microscopy (AFM) offers a number of distinct advantages over other morphological characterization techniques used to study apoptosis. AFM resolution is on the order of a few angstroms in the z

direction and x – y resolution for cell work has been reported as high as ~ 30 Å.^{13–15} In contrast to electron microscopy studies, this high degree of resolution can be obtained with cells supported on normal tissue culture plates and in typical cell growth media. Thus, the morphological changes associated with apoptosis can be followed for an individual cell over time in normal cell growth conditions in vitro.

A few AFM reports of apoptosis have already appeared in the literature. An early report by Kuznetsov et al. illustrated the classic blebbing morphology in an osteosarcoma cell undergoing apoptosis when the media became depleted in key factors needed for cell function.¹⁵ Girsole et al. observed a frictional contrast on the surface of fixed cells that had undergone apoptosis induced by interleukin-3.¹⁶ Despite these successes, the early progression of apoptotic volume decrease (AVD) has not been imaged by AFM and the associated volume and other morphology changes have not been quantified.

Many of the biochemical changes associated with apoptosis, such as changes in the cell membrane lipid composition, the mitochondrial membrane potential, DNA and activity of caspases are cell type and inducer specific. However, the loss of cell volume and the associated ion flux is a ubiquitous aspect of apoptosis.¹⁷ Many recent studies now suggest that apoptotic volume decrease (AVD) is not just a passive result of the biochemical changes occurring within the cell but that AVD plays an active and regulatory role in apoptosis.^{6,12,17–19} Although pre-

* To whom correspondence should be addressed.

[†] Department of Chemistry.

[‡] Department of Physics.

[§] Program in Applied Physics.

^{||} Program in Biophysics.

(1) Kerr, J. F. R.; Wyllie, A. H.; Currie, A. R. *Brit. J. Cancer* **1972**, *26*, 239–257.

(2) Lockshin, R. A.; Zakeri, Z.; Tilly, J. L. *When Cells Die: A Comprehensive Evaluation of Apoptosis and Programmed Cell Death*; John Wiley & Sons: New York, 1998.

(3) Bowen, I. D.; Bowen, S. M.; Jones, A. H. *Mitosis and Apoptosis*; Chapman & Hall: London, 1998.

(4) Hacker, G. *Cell Tissue Res.* **2000**, *301*, 5–17.

(5) Vu, C. C. Q.; Bortner, C. D.; Cidlowski, J. A. *J. Biol. Chem.* **2001**, *276*, 37602–37611.

(6) Maeno, E.; Ishizaki, Y.; Kanaseki, T.; Hazama, A.; Okada, Y. *Proc. Natl. Acad. Sci.* **2000**, *97*, 9487–9492.

(7) Orlov, S. N.; Dam, T. V.; Tremblay, J.; Hamet, P. *Biochem. Biophys. Res. Co.* **1996**, *221*, 708–715.

(8) Lang, F.; Ritter, M.; Gamper, N.; Huber, S.; Fillon, S.; Tanneur, V.; Lepple-Wienhues, A.; Szabo, I.; Gulbins, E. *Cell Physiol. Biochem.* **2000**, *10*, 417–428.

(9) Yu, S. P.; Canzoniero, L. M. T.; Choi, D. W. *Curr. Opin. Cell Biol.* **2001**, *13*, 405–411.

(10) Yu, S. P.; Choi, D. W. *Proc. Natl. Acad. Sci.* **2000**, *97*, 9360–9362.

(11) Okada, Y.; Maeno, E. *Comp. Biochem. Phys. A* **2001**, *130*, 377–383.

(12) Bortner, C. D.; Cidlowski, J. A. *Biochem. Pharmacol.* **1998**, *56*, 1549–1559.

(13) Nagao, E.; Dvorak, J. A. *J. Microsc. (Oxford)* **1998**, *191*, 8–19.

(14) Nagao, E.; Dvorak, J. A. *Biophys. J.* **1999**, *76*, 3289–3297.

(15) Kuznetsov, Y. G.; Malkin, A. J.; McPherson, A. *J. Struct. Biol.* **1997**, *120*, 180–191.

(16) Girasole, M.; Cricenti, A.; Generosi, R. *Appl. Phys. Lett.* **2001**, *78*, 1143–1145.

(17) Bortner, C. D. C.; J. A. *Cell Death Differ.* **2002**, *9*, 1307–1310.

(18) Hughes, F. M. B.; C. D., Jr.; Purdy, G. D.; Cidlowski, J. A. *J. Biol. Chem.* **1997**, *272*, 30567–30576.

vious research has shown that volume change and the accompanying ion flux is an early prerequisite of apoptosis,^{5,6,8-12} the techniques employed for evaluating the volume changes of live cells only measure the total volume change. The morphological details of the volume change are unknown and the exact order in which the biochemical and morphological changes occur is still a matter of debate.

Experiments conducted in our laboratory using AFM show KB cells experiencing dramatic morphological and volume changes within minutes of exposure to staurosporine, a nonspecific apoptosis-inducer. These results suggested we could test the following hypotheses: (1) staurosporine-induced AVD is rapid and occurs in equal proportion from the cytosol and the nucleus and (2) the volume and morphological changes during AVD occur before activation of key time-points defined by biochemical cascades. In the process of exploring these two hypotheses, a number of interesting morphological changes were observed that will also be discussed below.

To investigate these hypotheses, we have combined AFM, light and fluorescence microscopy, and cell flow cytometry data. AFM and light microscopy allow us to look at the morphological changes on a single cell basis with high resolution and as a population, respectively. The fluorescence microscopy and cell flow cytometry can be used to investigate when certain biochemical changes associated with apoptosis take place within the cell. The five biochemical time-points that were analyzed are phosphatidylserine (PS) translocation from the inner to the outer leaflet of the cell membrane, caspase 3 activation, change in mitochondrial membrane potential, DNA fragmentation, and nuclear condensation.

Experimental Section

Cell Growth. The KB cell line is a human epidermoid carcinoma. KB cells were chosen because they are a robust cell line and are very adherent, which is a requirement for AFM imaging of living cells. KB cells were purchased from the American Type Tissue Collection (ATCC, Manassas, VA, catalog number CCL-17) and grown continuously as a monolayer at 37 °C, and 5% CO₂ in RPMI 1640 medium. This medium was supplemented with penicillin (100 units/mL), streptomycin (100 mg/mL), 10% heat-inactivated FBS, and 25 mM HEPES. This media was used for all of the experiments discussed in this paper. Tissue culture treated Falconware Petri dishes were used for the growth and propagation of KB cells and are the typical substrate used for the cells when other assays of apoptosis were performed. For these reasons, they were an ideal substrate for use in the AFM imaging experiments.

AFM Measurements. All measurements were made using contact mode operation with a Digital Nanoscope IIIa Multimode scanning probe microscope from Veeco Instruments (Santa Barbara, CA) using a modified "J" vertical engage, vertical closed-loop scanner. The scanner was modified by Digital Instruments to achieve twice the z range normally available with a J scanner. This scanner underwent all of the same calibration procedures as any other scanner produced by Digital Instruments. The only difference between this modified J scanner and the unmodified version, other than the increase in z limit, is the decrease in overall lifetime of the piezo crystal. This means that the modified scanners must be replaced more frequently than the unmodified ones. However, with proper calibration, this modified scanner is as reliable and accurate as the standard J scanner available for this AFM. See Figure 1 in the Supporting Information for scanner height measurement accuracy and precision information. The modified scanner has a z range of 11 μm allowing the $\sim 9 \mu\text{m}$ tall KB cells to be imaged. Tapping mode was not used to obtain

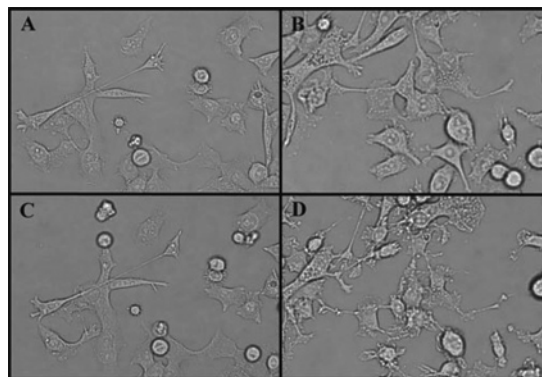


Figure 1. Brightfield light microscopy images show that most cells exposed to 1 μM staurosporine exhibit distressed, shrunken morphology after 3 h. (A) and (C) are untreated KB cells at time 0 and 3 h, respectively. (B) and (D) are KB cells treated with 1 μM staurosporine at time 0 and 3 h, respectively.

images due to observed lack of increase in spatial resolution and the longer image acquisition times required for this mode versus contact mode. During tapping mode, the entire liquid cell is being oscillated to oscillate the tip. This required us to image at much lower speeds to obtain stable images of cells. Images were obtained using sharpened, gold coated unmounted Microlevers from Veeco Metrology Group (Cat. # MSCT-AUNM). This probe contains 5 cantilevers (4 triangular, 1 plank shaped) on one side. Cantilever C, which has the smallest spring constant (0.01 N/m), was used to minimize the force applied to the cells. The set-point was set in the "Force Calibration" part of the software that allows us to set the imaging set-point to the minimum value required to image the sample. This minimizes the forces felt by the sample. All images presented were obtained from height mode data. Scanning Probe Image Processing (SPIP v2.1) software was employed for Figure 2 to show a 3-dimensional representation. Samples were prepared for imaging as follows. A total of 1×10^6 KB cells were plated and grown for 3 days in RPMI medium on tissue culture treated Falconware 35 mm Petri dishes, resulting in adherent cells that were slightly less than confluent. A 10 mm disk was punched from the center of the Petri dish, the cell growth media was replaced with fresh RPMI media, and the sample was transferred to the AFM. The temperature of the media in the AFM liquid cell is 28 °C as measured by a type-K thermocouple inserted into the media. Temperature was measured for a model experiment in which cells were not actually imaged and after imaging was ended for one of the cell experiments. Although this is not physiological temperature (37 °C), the cells are still viable at this temperature during the period of the AFM experiment. It is expected that some cellular processes would be slowed at this temperature, but the cell is still functional. Under these conditions, the control KB cells could be imaged for more than 5 h with no morphological changes measured by AFM or observed by optical microscopy. Apoptosis was induced by adding fresh RPMI media containing 1 or 2 μM staurosporine. Staurosporine was selected as the apoptosis induction agent for these studies because it is a common positive control and induces apoptosis in KB cells independent of cell cycle.²⁰

To determine the volume of the cells the image files were converted to ascii format using the instrument software and exported to MATLAB 7.0. A program developed in our lab was used to calculate the volume of each cell by integrating the volume of each height pixel. The first volume of the cell calculated in the first image of each experiment was set as 100%. The volume of the cell in subsequent images of each experiment are given as a percentage of the volume of the cell in the initial image.

Nucleus Volume Calculations. Confocal images of KB cells stained with Hoechst 33258 (staining procedure discussed below) were used to estimate the diameter of the nucleus. The confocal images were exported to Photoshop 7.0, and the percentage of the cell body area occupied by the nucleus was determined by comparing the number of pixels that were blue from the nuclear stain to the number of pixels for the whole cell in the image

(19) Dallaporta, B.; Hirsch, T.; Susin, S. A.; Zamzami, N.; Larochette, N.; Brenner, C.; Marzo, I.; Kroemer, G. *J. Immunol.* **1998**, *160*, 5605–5615.

(20) Swe, M.; Bay, B. H.; Sit, K. H. *Cancer Lett.* **1996**, *104*, 145–152.

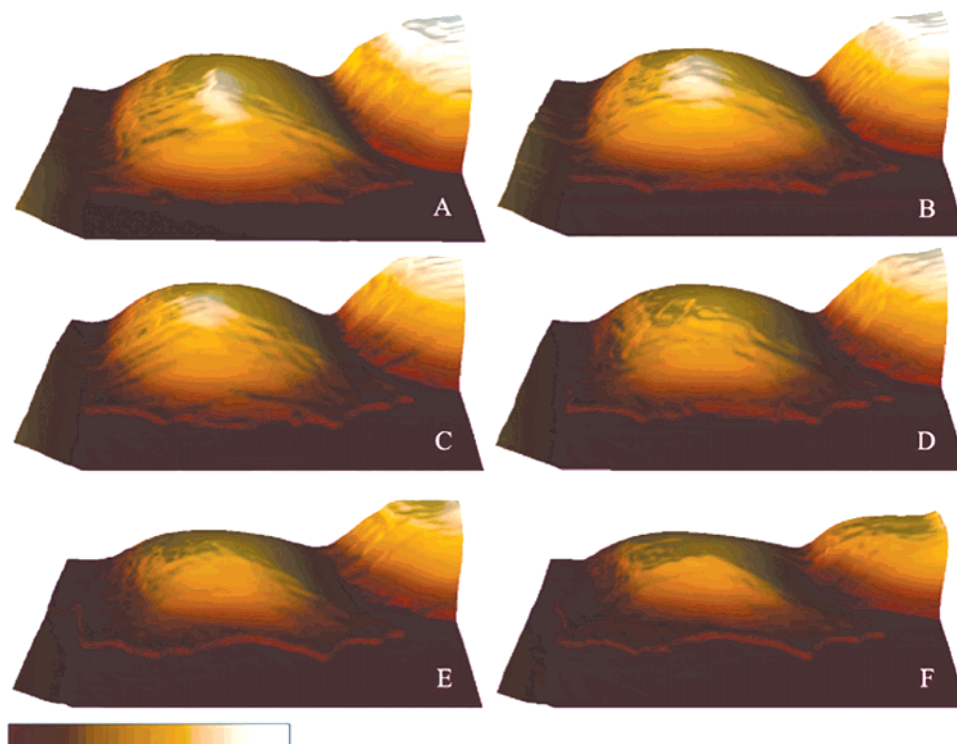


Figure 2. Height-mode AFM images of KB cells in RPMI 1640 media exposed to 1 μ M staurosporine. (A) before exposure; (B) 16 min after exposure to 1 μ M staurosporine; (C) 48 min after exposure; (D) 1 h 20 min after exposure; (E) 1 h 52 min after exposure; (F) 2 h 24 min after exposure. Images are 60 μ m \times 30 μ m. Vertical scale shown is from 0 to 9 μ m.

histogram. This process was repeated and an average obtained for seven cells in each confocal image (Figure 4, panels A and B), before and after exposure to drug, on cells that appeared to be well adhered. The average percent of cell area covered by the nucleus was $29 \pm 6\%$ and $24 \pm 6\%$ for the untreated cells and the cells treated with staurosporine, respectively. The initial and final AFM images corresponding to the same time-points as the confocal images were then exported to Photoshop and a circle was drawn to represent the nucleus that occupied the same percentage of the cell area as that measured for the confocal images. The radius of the drawn nucleus was then extrapolated from knowing the length scale for the AFM image. The height of the nucleus was obtained by measuring the tallest point in the AFM image that appeared to correspond to the nucleus (see linescans in Figure 3A). The nucleus was approximated three different ways: as a cone ($\frac{1}{3}\pi r^2 h$), half an oblate ellipsoid ($\frac{2}{3}\pi r^2 h$), and a spherical cap ($\frac{1}{6}\pi h(h^2 + \frac{3}{4}(2r)^2)$) (r = radius of the nucleus and h = height). The volume of the cytosol was then estimated by subtracting the calculated volume of the nucleus using each model from the volume measured by integration of the AFM images.

Phosphatidylserine (PS) Translocation. Analysis of the PS translocation was performed using the ApoAlertTM Annexin V-EGFP kit available from BD Biosciences, Clontech and analyzed using cell flow cytometry according to the manufacturer's instructions supplied with the kit. Approximately 500 000 KB cells were plated in 6 well plates in the aforementioned RPMI 1640 media. Positive control KB cells were incubated at 37 $^{\circ}$ C and 5% CO₂ with 1 μ M staurosporine for 6 h. Experimental wells were exposed to 1 μ M staurosporine for 3 h at ambient conditions before analysis to mimic the AFM experimental conditions. AFM experiments of KB cells typically lasted for 3–4 h after exposure to staurosporine before the cells released from the surface and could no longer be observed by AFM. The kit contains both Annexin V-EGFP and propidium iodide (PI). The Annexin V-EGFP selectively binds to PS in the membrane and fluoresces green. During the early stages of apoptosis, PS translocates from the inner leaflet of the membrane to the outer leaflet of the membrane. Thus, green fluorescence signals an early apoptotic cell. The PI intercalates with DNA and fluoresces red. The PI can only enter the cell if the integrity of the cell membrane has been compromised, such as in necrotic cells or in late apoptotic

cells. All cell flow cytometry samples were analyzed with a Beckman Coulter Epics XL-MCL flow cytometer and the data was analyzed with Expo 32 ADC analysis software.

Detection of Caspase 3 by Flow Cytometry. Caspase 3 is a common effector caspase that is activated during most forms of induced apoptosis. It therefore serves as a useful time-point in the apoptotic cascade.²¹ KB cells were grown in the aforementioned RPMI 1640 media overnight. Fresh media containing staurosporine at concentrations of 1, 2, and 4 μ M was then added. Cells were treated for 3 or 6 h at room temperature. After treatment, adherent cells were lifted and 10⁶ cells were transferred to a fresh tube. Cells were stained using the CaspaTag caspase 3 (DEVD) Activity Kit (Intergen Cat.# S7301) and incubated for 1 h at 37 $^{\circ}$ C and 5% CO₂ while being protected from the light. Cells were then washed twice in the washing buffer supplied by the manufacturer and resuspended in 400 μ L of the same solution. Immediately prior to flow cytometry analysis, cells were stained with propidium iodide. The number of caspase 3 positive cells and necrotic cells was determined by analyzing the cells with the previously mentioned cell flow cytometer and software. Cells that were positive for activated caspase 3 fluoresced green in the FL1 channel and necrotic cells fluoresced red in the FL3 channel. Red fluorescence is due to the intercalation of PI with DNA, and the green dye is a carboxyfluorescein analogue that is conjugated to an inhibitor of caspase 3 that binds irreversibly to the activated caspase.

Detection of Apoptosis by Analysis of Membrane Potential. The change in mitochondrial membrane potential has been shown to be related to the release of apoptogenic factors such as cytochrome c.²² KB cells were grown overnight in the same RPMI media as described in the previous section. The same concentrations of staurosporine were also used as in the previously described experiment. Cells were incubated 3–6 h at room temperature. After treatment, adherent cells were trypsinized and 10⁶ cells were transferred to a fresh tube. Cells were stained with MitoSensor dye from the ApoAlert Membrane Sensor Kit (CLONTECH Laboratories). Cells were suspended in the MitoSensor dye and incubated at 37 $^{\circ}$ C and 5% CO₂, while being

(21) Shi, Y. *Mol. Cell* **2002**, *9*, 459–470.

(22) Gottlieb, E.; Armour, S. M.; Harris, M. H.; Thompson, C. B. *Cell Death Differ.* **2003**, *10*, 709–717.

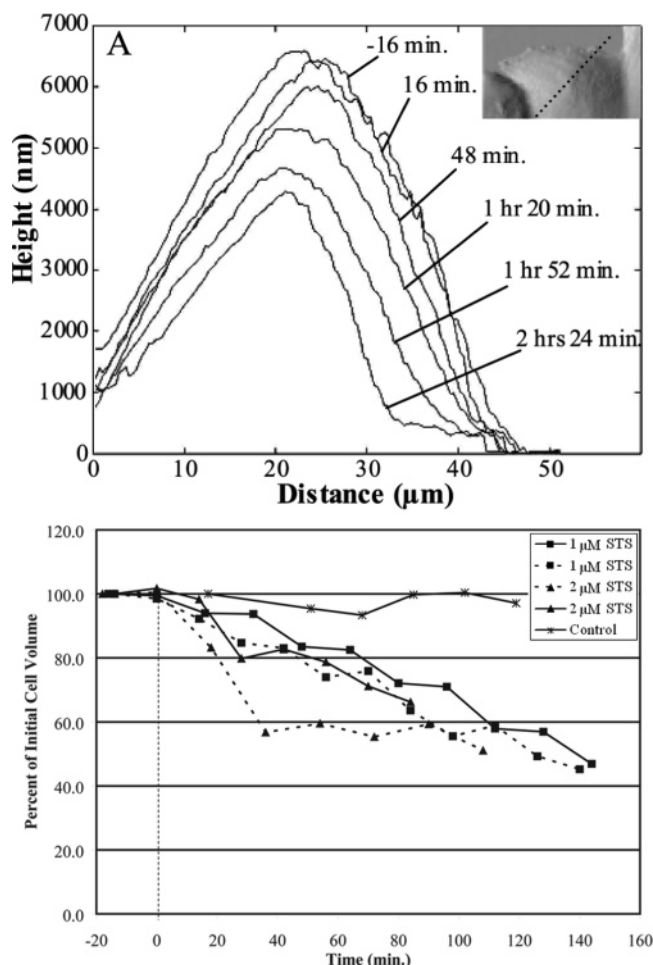


Figure 3. (A) Line scans for AFM images of KB cells shown in Figure 2 exposed to $1 \mu\text{M}$ staurosporine (STS). Line scans taken across dashed line shown in inset. (B) Graph of integrated volume change of KB cells exposed to staurosporine (STS) over time as percent of initial cell volume. Four individual experiments conducted under the same conditions are shown. Two experiments (square markers, solid and dashed line) show cell volume response to $1 \mu\text{M}$ STS and two experiments (triangle markers, solid and dashed line) show cell volume response to $2 \mu\text{M}$ STS. Solid line with asterisk shows cell volume over same length of time without the addition of drug. Negative time is before and positive time is after addition of STS. Solid line with square markers corresponds to cell shown in Figure 2 and line scans in panel A.

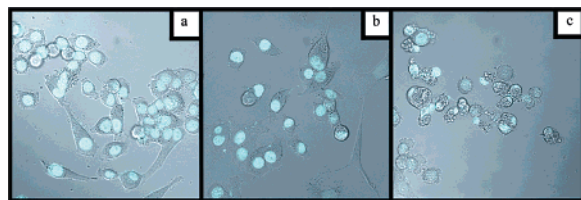


Figure 4. Confocal microscopy images of KB cells stained with Hoechst 33258 nuclear stain. (a) untreated KB cells, (b) and (c) KB cells exposed to $1 \mu\text{M}$ staurosporine for 3 and 5 h, respectively. Note that cells exposed for 5 h show blebbing (panel c), whereas cells exposed for 3 h do not (panel b).

protected from the light according to the instructions supplied by the manufacturer. Cells were washed and analyzed by flow cytometry. If cells are intact, the dye does not penetrate inside the mitochondria and the monomers of dye stay in the cytoplasm and fluoresce green. If the cells have entered the apoptotic stage, the dye accumulates and aggregates inside the mitochondria and fluoresces red. Samples were analyzed using the previously mentioned cell flow cytometer and software.

An experiment that mimicked AFM conditions was also conducted with the MitoSensor™ dye. Since the AFM experiments lasted 3–4 h, a 3 h time-point was chosen for the biochemical assays. A later time-point was also chosen to see if the cells that showed no biochemical change at 3 h showed changes at a later time-point. Cells were analyzed by flow cytometry at two time points, 3 and 12 h after exposure to staurosporine. 10^6 KB cells were plated in 6 well plates 1 day in advance. Before beginning the experiment, the cell media was aspirated and fresh RPMI 1640 was added to each well. Treated wells were exposed to RPMI 1640 media with $1 \mu\text{M}$ staurosporine. Cells were incubated at room temperature for the first 3 h to mimic the AFM conditions. At the 3 h time point, sample wells were divided into thirds. One-third was analyzed by flow cytometry, one-third was re-plated in fresh media, and one-third was re-plated in media with $1 \mu\text{M}$ staurosporine. These two latter cultures were analyzed at the 12 h time point. At the 12 h time point, this method resulted in cells that had been exposed to staurosporine for only 3 h and then exposed to untreated media for 9 h and cells that had been exposed for 12 continuous hours. Cells to be analyzed by flow cytometry were trypsinized and resuspended in PBS. The staining procedure suggested by the manufacturer and discussed above was then followed.

Optical Analysis of Morphological Change. KB cells were grown for 3 days using the aforementioned RPMI 1640 in a 24 well plate. To initiate apoptosis, fresh media containing staurosporine at concentrations of 1, 2, 4, 6, and $8 \mu\text{M}$ was then added and the morphological changes documented by taking brightfield light images using an Olympus IX-70 at $20\times$ magnification. The images were digitized using a Spot camera (Diagnostic Instruments).

DNA Content Analysis. The DNA content of KB cells exposed to staurosporine was analyzed by flow cytometry at 3, 48, 96, and 144 h time-points. The 3 h time-point was chosen to correlate with the AFM experiments. The other time-points were chosen after repeated attempts at this experiment to best illustrate the change in DNA content. These longer time-points also show the ability of many of the cells to recover once the staurosporine is removed. KB cells were plated in 6 well plates in RPMI 1640 media 1 day in advance. Before beginning the experiment, the media was aspirated and fresh RPMI 1640 was added to each well. Treated wells were then exposed to $1 \mu\text{M}$ staurosporine. At 3 h cells were trypsinized, centrifuged and resuspended in $500 \mu\text{L}$ media. Cells were centrifuged again. Cells to be measured by flow cytometry analysis for the 3 h time-point were re-suspended in 1 mL PBS. Cells to be measured by flow cytometry at later time-points were either re-suspended in 1 mL of untreated media or 1 mL of media treated with $1 \mu\text{M}$ staurosporine. At each time-point, cells resuspended in 1 mL of PBS were fixed in 70% cold ethanol and stored at -20°C . Samples were then prepared for flow cytometry analysis at the same time. For analysis, fixed samples were centrifuged, and the ethanol was removed. Subsequently, cells were resuspended in 1 mL of PBS and centrifuged. Cells were then suspended in $500 \mu\text{L}$ of extraction solution. The extraction solution consisted of extraction buffer and PBS in a 0.4 ratio. Extraction buffer consisted of 0.2 M anhydrous sodium phosphate monobasic (Sigma Cat.# 331988) and 0.004 M citric acid (Sigma Cat.# C0759) in Type 1 deionized water. Cells were incubated for 5 min at room temperature in the extraction solution and then centrifuged. Cells were then suspended in $100 \mu\text{L}$ of DNA staining solution. DNA staining solution consisted of 0.02 mg/mL propidium iodide (Sigma, Cat.# P4170) and 0.1 mg/mL RNase, DNase free (Roche, Cat.# 1579681) in PBS buffer. Staining solution should be prepared fresh on the day of analysis. Cells were incubated in the DNA staining solution for 30 min at room temperature, brought to a final volume of $500 \mu\text{L}$ with PBS buffer and then analyzed by flow cytometry. Control samples without staurosporine showed less than 5% of cells had apoptotic DNA.

Nuclear Condensation. Hoechst 33258 dye (Sigma-Aldrich, Cat.# 86,140–5) was used to analyze nuclear condensation after exposure to $1 \mu\text{M}$ staurosporine. KB cells were plated 1 day in advance on MatTek tissue culture dishes (glass bottom No. 15, uncoated, γ -irradiated, Part # P35G-1.5–10-C) in RPMI 1640 media. Cells were exposed to $1 \mu\text{M}$ staurosporine for 3, 5, and 24 h including 3 h of initial exposure at ambient conditions to

mimic AFM imaging conditions. Prior to analysis by confocal microscopy, the media was aspirated from each plate and 1 mL of RPMI 1640 containing 2 $\mu\text{g/mL}$ Hoechst 33258 was added. Cells were incubated for 30 min in the dark in the staining solution. The Hoechst staining solution was then aspirated and 2 mL of RPMI 1640 media was added to each plate. Samples were analyzed using a Zeiss 510 laser scanning confocal microscope. Cells were imaged using the appropriate filter for viewing Hoechst 33258 (Hoechst 364 nm @ 100% band-pass filter 385–470 nm).

Results and Discussion

The exposure of KB cells to 1 μM staurosporine resulted in a granular morphology within 3 h as imaged by light microscopy (Figure 1). Staurosporine is a nonselective inhibitor of a broad spectrum of kinases that blocks the binding of ATP to the kinase, thereby resulting in its inhibition. Staurosporine-induced apoptosis occurs through the mitochondrial caspase activation pathway, but its exact mechanism of induction is unknown.^{23–25} All of the cells showed signs of distress after the treatment, as expected based upon previous literature reports.²⁰ However, the details of the morphological change are not obvious in these optical images. In a parallel experiment, KB cells were imaged in contact mode by AFM during staurosporine treatment (Figure 2). Morphological change is apparent at the first time-point measured, 16 min after bathing the cell in the 1 μM staurosporine-containing media. In particular, the plateau that ultimately encircles the cell (Figure 2F) is already beginning to form. It is also apparent in this set of images that the cell height is already decreasing. This is significant because KB cells adopt a “fried egg” shape when adhered to plastic with the region of maximum height present over the cell nucleus. The immediate diminution in height raises the question of whether the structural integrity of the nucleus may be compromised in the earliest stages of AVD (*vide infra*). The change in cell height and the formation of the cell edge plateau are highlighted by the line scans provided in Figure 3A. The cell height changes from an initial value of 6.9 μm to a final value of 4.7 μm . The cell edge retracts approximately 5 μm or $\sim 15\%$ of the initial cell diameter. At the same time, a roughly 10 μm wide plateau forms on the edge of the cell that is 0.2–0.5 μm in height. The morphological and volume changes observed by AFM were consistent through four separate experiments under identical conditions at two different concentrations of staurosporine, 1 and 2 μM . The images shown are a typical representation of these changes.

To assess the magnitude of the AVD associated with the changes in height and cell shape, we have integrated the volume under the topographical map of the cell measured at each time point for cells exposed to 1 and 2 μM staurosporine and cells exposed to no drug. As is illustrated in Figure 3B, the total cell volume decreases smoothly over the 2–3 h time period that the cells are imaged, resulting in a 50% loss of cell volume for all cells except the control cells that were not exposed to drug. The control line in Figure 3B shows that cell volume as observed by AFM does not change by more than 5%. Figure 3B shows that the cell responds within a matter of minutes to the presence of staurosporine but that the total volume loss occurs slowly over a few hours. At this time, the cell

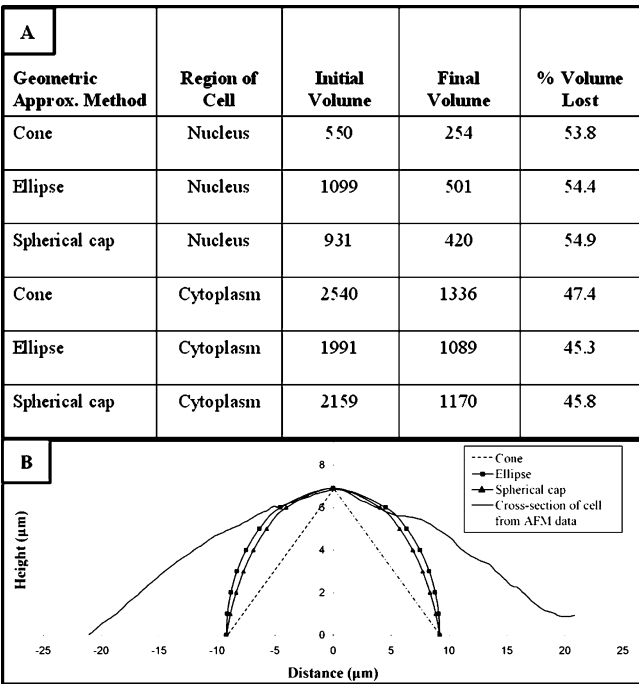


Figure 5. (A) Calculated volumes for the nucleus and the cytoplasm before and after exposure to staurosporine using three geometric approximation models. (B) Cross-section of the AFM image of a cell overlaid with the three models used to approximate the volume of the nucleus.

releases from the surface and can no longer be imaged by AFM. As noted above, the diameter of the cell decreases by 10–20% over this time period.

The rapid change in height observed by AFM after exposure to staurosporine brings up an interesting question of whether the volume loss is due to dramatic changes in the nucleus alone or from a decrease in all areas of the cell. The AFM does not allow us to see inside the cell; however, if we make 2 assumptions about the shape of the nucleus, we can use the AFM data in combination with confocal microscopy to estimate whether the volume change is due to dramatic changes in one area of the cell or an overall change in the entire cell. One assumption is that the nucleus is symmetrical. The other assumption is that the amount of volume present between the top of the nucleus and the top of the whole cell as determined by AFM is negligible compared to the volume of the nucleus and whole cell. Confocal images of KB cells stained with the nuclear dye Hoechst 33258 were used to estimate the volume of the nucleus before and after exposure to staurosporine using the spherical cap model (Figure 4, panels A and B). The height of the nucleus at each time-point was determined directly from the linescans of the AFM data (Figure 3A). The volume for the nucleus was then estimated as described in the Experimental Section using three different models. The volume for the whole cell was obtained by integrating under the topographical map of the images obtained by AFM as described above. The volume of the cytoplasm was estimated by subtracting the estimated nuclear volume from the cell volume measured by AFM. The calculated volumes for the nucleus and the cytoplasm using all three geometric models to approximate the nucleus are shown in Figure 5A. The cone model for the nucleus is very simple and underestimates the volume of the nuclei, whereas the elliptical and spherical cap models may overestimate the volumes at the edges, as illustrated in Figure 5B. However, assuming the nucleus maintains its symmetry throughout the experiment, we can compare the ratio of the volumes

(23) Takahashi, A.; Hirata, H.; Yonehara, S.; Imai, Y.; Lee, K. K.; Moyer, R. W.; Turner, P. C.; Mesner, P. W.; Okazaki, T.; Kishi, S.; Yamamoto, K.; Okuma, M.; Sasada, M. *Oncogene* **1997**, *14*, 2741–2752.
(24) Stepczynska, A.; Lauber, K.; Engels, I. H.; Janssen, O.; Kabelitz, D.; Wesselborg, S.; Schulze-Osthoff, K. *Oncogene* **2001**, *20*, 1193–1202.
(25) Bertrand, R.; Solary, E.; O'Connor, P.; Kohn, K. W.; Pommier, Y. *Expt. Cell Res.* **1994**, *211*, 314–321.

before and after exposure to the drug to determine how much volume is lost as a percentage of the initial volume. Using the calculated volumes from all three models, the nucleus appears to have lost ~55% of its initial volume after exposure to 1 μ M staurosporine, whereas the cytoplasm lost ~45% of its initial volume. The calculated change in volume of the nucleus is independent of the geometric model chosen. These calculations suggest that the decrease in cell volume after exposure to staurosporine is occurring throughout the entire cell, nucleus, and cytoplasm, rather than disproportionally from a specific area.

The AFM and optical microscopy images indicate the cell volume loss occurs prior to blebbing. During the AFM experiment, the cell surface appears fairly smooth. There is no evidence of the cell blebbing or membrane budding that occurs during apoptosis. Blebbing is proposed to occur at places of weakness between the actin cytoskeleton and the cell membrane. These areas of weakness allow small packets of membrane to protrude from the cell surface. Eventually these membrane buds pinch off and are engulfed by neighboring cells.²⁶ The model put forward by Mills et al. suggests that, as the cell enters the apoptotic pathway, it first rearranges its focal adhesions to the surface and takes on a more rounded appearance. This is followed by the onset of cell blebbing which ultimately leads to a shrunken cell. Our results differ from both of these proposals. If blebbing was occurring, the AFM images would not appear smooth but would appear rough and streaky due to the rapid change in cell height as blebs were formed and released. Typical linescan rates for imaging cells of this size are around 0.1–0.2 Hz. The scan rate for the experiment shown was 0.13 Hz, with a 1:2 aspect ratio. This means that each image took approximately 16 min to complete and each line took approximately 3.8 s. At these rates, a rapidly changing cell surface would have severely hampered our ability to obtain stable images of the cell over a long period of time. The light microscopy images in Figure 1 also show no signs of blebbing after 3 h of exposure to staurosporine. In Figure 4B, cells exposed to 1 μ M staurosporine do not show signs of blebbing by confocal microscopy; however, by 5 h (Figure 4C), all of the cells visible are blebbing. These results suggest that blebbing does not occur during the early stages of apoptosis in this system and are not associated with the decrease in cell volume. Our results also show that the cell does not round up and rearrange its focal adhesions prior to volume loss. It first decreases in volume before significant change in cell footprint occurs.

To assess the second hypothesis, biochemical assays were performed to correlate the morphological changes imaged by AFM with well-documented time-points in the biochemical cascade of apoptosis.^{27–30} The AFM data shows the cells losing almost half of their initial volume within 3 h of exposure to 1 μ M staurosporine, at which point the cells lift off the surface. The biochemical assays allow correlation of the volume change that begins minutes after exposure to staurosporine to the chemical changes taking place within the cell. The five time-points that were analyzed were the phosphatidylserine (PS) translocation from the inner to the outer leaflet of the cell membrane,

caspase 3 activation, change in mitochondrial membrane permeability, DNA fragmentation, and nuclear condensation.

Analysis of the PS flip was performed using the ApoAlert™ Annexin V-EGFP kit available from BD Biosciences, Clontech and analyzed using flow cytometry. KB cells were incubated at 37 °C and 5% CO₂ with 1 μ M staurosporine for 6 h. Flow cytometry analysis showed Annexin-EGFP was bound to 33 \pm 5% of the cells, indicating the PS of these cells had translocated from the inner leaflet of the membrane to the outer leaflet and that these cells were apoptotic. KB cells that were exposed to 1 μ M staurosporine for 3 h under conditions identical to the AFM experiment, i.e., ambient conditions, showed no increase in PS exposure as analyzed by flow cytometry compared to the untreated control (data not shown). The data suggests that the volume changes observed by AFM after exposure to staurosporine precede the PS translocation to the outer leaflet of the membrane.

Caspase 3 activation was determined by flow cytometry analysis using the CaspaTag caspase 3 (DEVD) activity kit from InterGen. Caspases, especially caspase 3, are activated in the protease cascade that occurs during apoptosis that leads to the activation or inactivation of key structural proteins and signaling and repair enzymes that are necessary for the destruction of the cell. Caspase 3 is often activated, but its necessity for the morphological changes that occur during apoptosis is unknown.³¹ KB cells were exposed to 1, 2, and 4 μ M staurosporine for 3 h at room temperature. Cells exposed to 1 μ M staurosporine showed no significant increase in caspase 3 activity over that of untreated cells. Staurosporine exposure at 2 μ M showed a 20% increase in caspase 3 activity over untreated cells after 3 h. To the limit of our detection capability, caspase 3 is not active before or during the initial volume decrease of the cells. This suggests that the cellular proteins that are cleavage substrates for active caspase 3 are not involved in the volume and morphological changes in the early stages of apoptosis.

The change in mitochondrial membrane potential was assessed using the ApoAlert Membrane Sensor Kit and analyzed by flow cytometry analysis. KB cells were exposed to 1 μ M staurosporine and analyzed at two different time points, 3 and 12 h. At the 3 h time point, cells exposed to 1 μ M staurosporine for 3 h showed no change in mitochondrial membrane potential relative to the untreated control measured by green fluorescence. At the 12 h time point, KB cells exposed to 1 μ M staurosporine continuously for 12 h exhibited an average increase in green fluorescence of 15 \pm 5% over untreated controls. This correlates to an increase in depolarized mitochondrial membranes. KB cells that were treated with 1 μ M staurosporine for 3 h and then exposed to staurosporine-free media and analyzed by flow cytometry 9 h later showed an average increase in green fluorescence over untreated controls of 14 \pm 1%. Taken together, the flow cytometry and AFM results suggest that the volume changes observed by AFM within minutes of exposure to staurosporine precede changes in the mitochondrial membrane potential. The results also suggest that the cells observed to lose volume by AFM will eventually undergo later stages in the apoptotic process such as a change in the mitochondrial membrane potential.

As noted earlier, the decrease in cell height raises the question of nuclear integrity during the early stages of AVD. To address this question, DNA fragmentation was analyzed using a Hoechst 33258 stain. The DNA content

(26) Mills, J. C.; Stone, N. L.; Pittman, R. N. *J. Cell Biol.* **1998**, *146*, 703–707.

(27) Ferri, K. F.; Kroemer, G. *Nat. Cell Biol.* **2001**, *3*, E255–E263.

(28) Chang, H. Y.; Yang, X. *Microbiol. Mol. Biol. Rev.* **2000**, *821*–846.

(29) Saraste, A.; Pulkki, K. *Cardiovasc. Res.* **2000**, *45*, 528–537.

(30) Hengartner, M. O. *Nature* **2000**, *407*, 770–776.

(31) Porter, A. G.; Janicke, R. U. *Cell Death Differ.* **1999**, *6*, 99–104.

analysis is also useful in assessing if the cell is committed to apoptosis.

Nuclear fragmentation, as indicated by DNA content within the cell was analyzed by flow cytometry using a propidium iodide stain. Cells containing fragmented DNA appear below the G1 peak (sub-G1/apoptotic cells) in the flow cytometry analysis. The DNA content of KB cells exposed to 1 μ M staurosporine was analyzed by flow cytometry at time points of 3, 48, 96, and 144 h. At each time point, samples were either exposed to staurosporine for 3 h and then transferred to untreated media for the remainder of the time or left exposed to staurosporine for the entire time. Cells that were exposed to staurosporine continuously showed an increase in sub-G1 fluorescence over the course of 144 h ultimately resulting in greater than 84% apoptotic cells (data not shown, untreated controls showed less than 6% of cells were apoptotic). Cells exposed to 1 μ M staurosporine for 3 h and then incubated in fresh media without staurosporine for the remaining time showed a small increase in sub-G1 fluorescence from 5% to 10%. However, many cells recovered by 144 h as shown by flow cytometry analysis and light microscopy. Two points can be inferred from the DNA content results. First, the decrease in volume observed by AFM after exposure to staurosporine precedes DNA fragmentation. Second, the DNA content data suggests that the cell shrinkage observed by AFM is reversible and does not by itself commit a cell to death.

Nuclear fragmentation was also assessed using Hoechst 33258 dye to determine if the dramatic decrease in height and volume observed by the AFM after exposure to staurosporine corresponds to loss of nuclear membrane integrity. KB cells were exposed to 1 μ M staurosporine for 3 or 5 h and then exposed to Hoechst dye and analyzed by confocal microscopy. The confocal microscopy of cells exposed for 3 h shows that the cells look similar to untreated cells in terms of localization of the dye (Figure 4B). At 3 h the nuclear envelope is intact and nuclear condensation has not begun. After 5 h of exposure to staurosporine, nuclear condensation can be seen in

approximately 30% of cells and all cells show signs of blebbing (Figure 4C). The confocal data taken together with the AFM results suggests that nuclear shape (i.e., height) can decrease significantly without nuclear condensation or loss of nuclear membrane integrity.

In summary, cell morphology changes associated with staurosporine-induced AVD have been quantified as a function of time in vitro using AFM. From the AFM images, it appears that the AVD occurs in equal proportion from the nucleus and the cytoplasm. The cell shrinkage results in the formation of a thin plateau around the cell edge as the volume decreases that is not visible employing standard light microscopy techniques. The combination of AFM and light microscopy data also shows that cell membrane blebbing is not occurring during the early AVD observed by AFM and is therefore not responsible for the volume loss that occurs. Cell flow cytometry shows that the morphological and volume changes observed by AFM precede later hallmarks of the biochemical cascade such as PS translocation, change in mitochondrial membrane potential, caspase 3 activation, and nuclear fragmentation and condensation. DNA content analysis also showed that the volume change alone is not enough to commit a cell to apoptosis. Confocal imaging of the stained nuclei showed that the nucleus remains intact during the initial stages of AVD observed by AFM.

Acknowledgment. The authors thank Mahesh Shenai, Damian Khan, and Yunqing Chen for many fruitful discussions on image analysis. This work is supported by the National Cancer Institute, National Institutes of Health (Contract No. NOI-CO-97111) and the University of Michigan, Ann Arbor.

Supporting Information Available: Scanner height measurement accuracy and precision information (Figure 1). This material is available free of charge via the Internet at <http://pubs.acs.org>.

LA051837G